ALEPH 98-22
CONF 98-12
6th March 1998

Production of $D_{s1}^{\pm}$ and $D_{s2}^{*\pm}$ mesons in hadronic Z decays

ALEPH Collaboration

PRELIMINARY

Abstract:

In a sample of 4.1 million hadronic Z decays recorded in the years 1991 to 1995 $D_{s1}^{\pm}$ and $D_{s2}^{*\pm}$ mesons are observed in the decay channels $D_{s1}^{+}\to D^{*0}K^{+}$, $D_{s1}^{+}\to D^{*+}K_S^0$ and $D_{s2}^{*+}\to D^0K^+$. Assuming that the decay width of the D_{s1}^{+} meson is saturated by the two measured decays and that the branching ratio $D_{s2}^{*+}\to D^0K^+$ is 45%, the total production rates for $x_E > 0.3$ in hadronic events are found to be:

$$n(Z^0 \to D_{s1}^{\pm})_{x_E(D_{s1}^{\pm})>0.3} = (0.41 \pm 0.08_{stat} \pm 0.06_{syst}) \cdot 10^{-2}$$
$$n(Z^0 \to D_{s2}^{*\pm})_{x_E(D_{s2}^{*\pm})>0.3} = (0.84 \pm 0.22_{stat} \pm 0.15_{syst}) \cdot 10^{-2}$$

The production rates of $D_{s1}^{\pm}$ and $D_{s2}^{*\pm}$ from charm quark fragmentation and from decays of b hadrons are derived from the observation in c and b enriched event samples. The Monte Carlo is used to subtract the remaining fraction of D_s^{**} mesons from other flavors and to extrapolate to the full energy region. The values obtained are:

$$n(c \to D_{s1}^{\pm}) = (0.77 \pm 0.20_{stat} \pm 0.08_{syst}) \cdot 10^{-2}$$
$$n(c \to D_{s2}^{*\pm}) = (1.3 \pm 0.5_{stat} \pm 0.2_{syst}) \cdot 10^{-2}$$
$$n(b \to D_{s1}^{\pm}) = (1.1 \pm 0.3_{stat} \pm 0.2_{syst}) \cdot 10^{-2}$$
$$n(b \to D_{s2}^{*\pm}) = (2.2 \pm 0.8_{stat} \pm 0.5_{syst}) \cdot 10^{-2}$$

ALEPH contribution to 1998 winter conferences

Contact Person: Eric Rohne (eric.rohne@cern.ch)

1 Introduction

In addition to the pseudoscalar and vector mesons $D_s^{\pm}$ and $D_s^{*\pm}$ also four orbitally excited $D_s^{**\pm}$ mesons with angular momentum L=1 exist. In the framework of HQET the spin of the light quark couples with the orbital angular momentum to $j = \frac{1}{2}$ or $j = \frac{3}{2}$. Taking the spin of the heavy quark into account one gets one ($j = \frac{1}{2}$) doublet with the quantum numbers $J^P = 0^+, 1^+$ and one ($j = \frac{3}{2}$) doublet with the quantum numbers $J^P = 1^+, 2^+$. These states are expected to decay mainly into (D,K) or (D^*,K) modes.
Spin and parity conservation allow only certain decays in S-wave or D-wave modes. The states of the ($j = \frac{1}{2}$) doublet decay via S-wave decays and are therefore expected to be broad ($\Gamma > 100$ MeV) and are not yet observed. The ($j = \frac{3}{2}$) doublet states are much more narrow since they can only decay via D-wave decays. The two narrow states $D_{s1}^{\pm}$ and $D_{s2}^{*\pm}$ have been observed by CLEO and ARGUS [1, 2, 3]. At LEP $D_{s1}^{\pm}$ mesons first have been observed by OPAL [5]. The properties of the four D_s^{**} states are listed in Table 1.
In this analysis the production rates of the two narrow states are measured in the decay modes $D_{s1}^{+} \to D^{*+}K^0$, $D_{s1}^{+} \to D^{*0}K^+$and $D_{s2}^{*+} \to D^0K^+$. In $Z \to c\bar{c}$ events D_s^{**} mesons are produced in the fragmentation of primary c quarks whereas in $Z \to b\bar{b}$ events they can only be produced in decays of b hadrons. To measure these two contributions independently the production rates are also obtained from b and c enriched event samples from which the fraction of D_s^{**} mesons from other flavors determined from Monte Carlo is subtracted.

	D^0,K^+	D^+,K^0	D^{*0},K^+	D^{*+},K^0	
D_{s1}^{+} $(J^P = 1^+)$	forbidden	forbidden	D-wave	D-wave	$m = 2535.3 \pm 0.3$ MeV $\Gamma < 2.3$ MeV
D_{s0}^{*+} $(J^P = 0^+)$	S-wave	S-wave	forbidden	forbidden	$\Gamma > 100$ MeV
D_{s1}^{*+} $(J^P = 1^+)$	forbidden	forbidden	S-wave	S-wave	$\Gamma > 100$ MeV
D_{s2}^{*+} $(J^P = 2^+)$	D-wave	D-wave	D-wave	D-wave	$m = 2573.5 \pm 1.7$ MeV $\Gamma = 15^{+5}_{-4}$ MeV

Table 1: Properties of D_s^{**} mesons

2 Event Selection and Detector Information

2.1 Event and Track Selection

In this analysis all preselected hadronic events taken at the Z peak in the years 1991-1995 are used. The selected runs are required to have a working VDET (**V**ertex **Det**ector), TPC (**T**ime **P**rojection **C**hamber) and ECAL (**E**lectromagnetic **Cal**orimeter). In total 4175240 events are selected. For charged tracks used in the analysis the cosine of the

angle to the beam axis has to be smaller then 0.95. The track has to have more than 3 hits in the TPC (**T**ime **P**rojection **C**hamber) and the χ^2 per degree of freedom of the helix track fit has to be smaller than 3. Finally the distance to the primary vertex in the xy-plane has to smaller than 2 cm and in z-direction smaller than 10 cm.

2.2 Kaon and Pion Separation with the Help of the Specific Ionisation Measurement (dE/dx)

The identification of charged tracks plays an important role in this analysis. For the separation of charged kaon and pion tracks the specific ionisation measurement (dE/dx) inside the TPC is used. For each charged track the measured dE/dx value μ is compared with the expected dE/dx for a pion and a kaon hypothesis and the pion and kaon estimators r_π and r_K are calculated

$$r_K = \frac{\mu - (dE/dx)_K}{\sigma} \qquad r_\pi = \frac{\mu - (dE/dx)_\pi}{\sigma}.$$

To identify a charged track as a pion $|r_\pi|$ has to be smaller than 2.5. Tracks with no dE/dx information are accepted as pions because requiring dE/dx information for all tracks would cause a significant drop in efficiency. To identify a particle as a kaon, $|r_K|$ has to be smaller than 2.5. In addition $|r_\pi|$ has to be bigger than 0.5 to suppress pion background.

2.3 The use of the Vertex Detector for b selection

The Vertex Detector (VDET) plays a central role in b identification since it allows precise determination of secondary vertices. It is therefore interesting to have in mind some of its characteristics. Surrounding the beam pipe, the VDET consists of two concentric layers of double-sided silicon detector, positioned at average radii of 6.5 cm and 11.3 cm, and covering respectively 85% and 69% of the solid angle. The spatial resolution of the VDET is 12 μm in $r\phi$ and between 12 μm and 22 μm for the z coordinate, depending on the polar angle of the track.

3 Decay Channel $\mathbf{D}^+_{s1}\rightarrow\mathbf{D}^{*+}\mathbf{K}^0_S$

K^0_S mesons are reconstructed in the decay channel $K^0_S\rightarrow\pi^+\pi^-$. For the identification of the K^0_S their long lifetime ($c\tau$ = 2.7cm) is exploited and for the reconstruction only neutral vertices with a distance of at least 1.5 cm to the primary vertex are used.
D^{*+} mesons are reconstructed in the decay channel $D^{*+}\rightarrow D^0\pi^+$and D^0 mesons are reconstructed in the four decay channels ($D^0\rightarrow K^-\pi^+$), ($D^0\rightarrow K^0\pi^+\pi^-$), ($D^0\rightarrow K^-\pi^+\pi^-\pi^+$) and ($D^0\rightarrow K^-\pi^+\pi^0$). The most important cuts for the suppression of combinatorial background are momentum cuts on the D^0 decay tracks. The remaining tracks are fitted to a common vertex and the χ^2 of the vertex fit has to be smaller than 20. To avoid

double counting in the decay channels with charged kaons and pions, the track with the lowest value of r_K is assumed to be the kaon track. Because the combinatorial background is mainly suppressed by the good resolution in the reconstruction of $D^{*\pm}$ mesons the cuts for the selection of D^0 mesons are rather loose. In the decay channel $D^0 \to K^-\pi^+\pi^0$ the momentum of the π^0 is calculated by a mass-constrained fit to the detected photons in the ECAL (**E**lectromagnetic **Cal**orimeter). The selected D^0 candidates are combined with all charged pions in the event and the mass difference $\Delta M_1 = m(D^0,\pi^+)$ - $m(D^0)$ is calculated. Subtracting the measured mass of the D^0 candidate improves the mass resolution for the $D^{*\pm}$ mesons. The number of reconstructed $D^{*\pm}$ mesons with momentum greater than 9 GeV/c is determined with a χ^2 fit to the measured ΔM_1 distributions in which the signal contribution is described by a Breit Wigner function. Table 2 shows the number of reconstructed $D^{*\pm}$ mesons in the different D^0 decay modes found in data. All

	$D^0 \to K^-\pi^+$	$D^0 \to K^0\pi^+\pi^-$	$D^0 \to K^-\pi^+\pi^-\pi^+$	$D^0 \to K^-\pi^+\pi^0$
$n(D^{*\pm})$	$6140 \pm 76_{stat}$	$1430 \pm 30_{stat}$	$3660 \pm 95_{stat}$	$5553 \pm 150_{stat}$

Table 2: Results of the fit to the $D^{*\pm}$ mass distributions in data.

$D^{*\pm}$ candidates in the mass window ± 1.5 MeV/c^2 around the central mass are combined with all K^0_S candidates with momentum greater than 2.5 GeV/c. The combination of the $D^{*\pm}$ and the K^0_S is required to have a scaled energy greater than 0.3. To improve the mass resolution the mass difference $\Delta M_2 = m(D^{*+},K^0_S) - m(D^{*+}) - m(K^0_S) + m_{true}(K^0_S)$ is calculated, where $m_{true}(K^0_S)$ is the nominal K^0_S mass. The mass difference distribution ΔM_2 for data is shown in Fig. 1. The distribution shows an excess of events in the signal region at 525 MeV/c^2. The combinatorial background is determined with the help of $D^{*\pm}$ candidates from sidebands above the $D^{*\pm}$ mass window. The width of the sidebands is chosen in a way to have approximately the same number of entries in the signal and the sideband window. The background shape is parametrized with the following function:

$$\frac{dN}{d(\Delta M)} = n \cdot (\Delta M - a)^b \cdot e^{-c(\Delta M - a)}$$

The number of signal events is determined with an unbinned likelihood fit to the signal and background distributions simultaneously. The signal is fitted with a Breit Wigner function which is convoluted with the detector resolution. The detector resolutions for the reconstruction of $D^{\pm}_{s1}$ mesons in the different D^0 decay channels are determined from Monte Carlo events. The results are shown in Table 3. The results of the fit to the ΔM_2 distribution are shown in Table 4. The systematic errors are due to a variation of the fit parameters. The width of the Breit Wigner function is varied between 0.5 and 2.5 MeV to take into account the uncertainty in the natural width of the $D^{\pm}_{s1}$ meson and the detector

$D^0 \to K^-\pi^+$	$D^0 \to K^0\pi^+\pi^-$	$D^0 \to K^-\pi^+\pi^-\pi^+$	$D^0 \to K^-\pi^+\pi^0$
1.6 ± 0.1 MeV/c^2	1.4 ± 0.1 MeV/c^2	1.7 ± 0.1 MeV/c^2	2.1 ± 0.2 MeV/c^2

Table 3: Detector resolutions for $D^+_{s1} \to D^{*+}K^0_S$ in the different D^0 decay channels

Decay channel	Fit results
$D_{s1}^{+} \to D^{*+} K_S^0$	n(D_{s1})=$25.1 \pm 6.1_{stat} \pm 2.4_{syst}$ mean=$525.6 \pm 1.0_{stat} \pm 1.0_{syst}$ MeV/c^2

Table 4: Results of the fit to the ΔM_2 distribution in data.

resolution is varied by $\pm 10\%$.
Adding the D^{*+} mass of (2010.0 ± 0.5) MeV/c^2 to the mean value of the fitted signal function one gets a mass of (2535.6 ± 1.0) MeV/c^2 for the mass of the D_{s1}^{+} meson, which is in good agreement with the value of (2535.35 ± 0.34) MeV/c^2 given in [4].

4 Decay Channels $D_{s1}^{+} \to D^{*0} K^{+}$ and $D_{s2}^{*+} \to D^0 K^{+}$

D^{*0} mesons decay into a D^0 by emitting a π^0 or a photon. The π^0 and the photon are not reconstructed in this analysis due to the low reconstruction efficiency for low momentum photons and pions. Instead the combination of the D^0 with all charged kaons in the event with momentum greater than 3 GeV/c is taken and the mass difference $\Delta M_3 = m(D^0,K^+)$-$m(D^0)$ is calculated. Because of the low Q-value in the decay $D^{*0} \to D^0 \pi^0$ of only 7 MeV/c^2 this does not significantly worsen the resolution which is determined to be (2.9 ± 0.1) MeV/c^2 from Monte Carlo. In the case where the D^{*0} emits a photon the resolution is (7.1 ± 0.2) MeV/c^2.
D_{s2}^{*+} mesons are allowed to decay directly into the (D^0,K) final state and therefore the mass difference ΔM_3 is also used to measure the decay $D_{s2}^{*+} \to D^0 K^+$. The detector resolution in the reconstruction of this decay is (3.1 ± 0.1) MeV/c^2 . The decay $D_{s2}^{*+} \to D^{*0} K^+$ is also allowed but suppressed due to lower phase space.
Because of the higher background in these channels the selection of D^0 candidates has to be more restrictive than for D^0 candidates used in the reconstruction of $D^{*\pm}$ mesons. The best signal to background ratio is achieved in the decay channel ($D^0 \to K^- \pi^+$) and therefore only this channel was used for the analysis. To get rid of D^0 mesons which are coming from D^{*+} decays only D^0 candidates are taken for which the combination with each π^+ in the event the mass difference $m(D^0,\pi^+)$-$m(D^0)$ is more than 2 MeV/c^2 away from the value expected for $D^{*\pm}$ decays. In addition to higher momentum cuts on the decay tracks of the D^0 of 3 GeV/c also the lifetime of D^0 mesons is exploited and D^0 vertices are required to have a distance of at least 0.5 mm to the primary vertex. This cut removes mainly combinatorial background which is peaked at lower distances to the primary vertex. The scaled energy of the (D^0,K) combination has to be greater than 0.3. The number of D^0 mesons in data is determined with a χ^2 fit of a Gaussian signal and a linear background function to the measured distribution. In total $(15500 \pm 190_{stat})$ D^0 mesons with momentum greater 9 GeV/c are found in data.
The mass difference distribution $\Delta M_3 = m(D^0,K^+)$-$m(D^0)$ in data for (D^0,K) combinations with a scaled energy greater than 0.3 is shown in Fig. 1. An excess of events is seen at 530 MeV/c^2 which is due to the decay $D_{s1}^{+} \to D^{*0} K^+$. The excess at 710 MeV/$c^2$

is due to the decay $D_{s2}^{*+} \to D^0 K^+$. The combinatorial background is determined with the help of the wrong-sign combinations (D^0,K^-). The shape of the combinatorial background for the decay of the D_{s1}^+ is parametrized with the same function given in paragraph 3. The combinatorial background for the decay of the D_{s2}^{*+} is described by a linear function. The contributions from reflections from the decays $D_1^+ \to D^{*0}\pi^+$ and $D_2^{*+} \to D^0\pi^+$ determined from Monte Carlo are also plotted. The number of signal events is determined with an unbinned likelihood fit to the signal and background distribution simultaneously. The signal is fitted with a Breit Wigner function convoluted with the Gaussian detector resolution. The systematic error is determined by a variation of the fit parameters. For the D_{s1}^+ the width of the Breit Wigner is varied between 0.5 and 2.5 MeV/c^2 and the position of the peak is varied by ± 1 MeV/c^2 around the value expected from Monte Carlo. For the D_{s2}^{*+} the width is varied between 10 and 20 MeV/c^2 and the position of the peak by ± 2 MeV/c^2. The detector resolution in both cases is varied by $\pm 10\%$. The results of the fit to the ΔM_3 distributions are shown in Table 5.

Decay channel	Fit results
$D_{s1}^+ \to D^{*0}K^+$	$n(D_{s1}^{\pm}) = 42.6 \pm 11.5_{stat} \pm 6.8_{syst}$
$D_{s2}^{*+} \to D^0 K^+$	$n(D_{s2}^{*\pm}) = 70.2 \pm 18.2_{stat} \pm 12.1_{syst}$

Table 5: Results of the fit to the ΔM_3 = m(D^0,K^+)-m(D^0) distribution in data.

5 Production Rates $c \to D_s^{**}$

Monte Carlo predicts that in the sample selected with the cuts described in the previous paragraph approximately 60% of the reconstructed D_s^{**} mesons are produced in $Z \to c\bar{c}$ events and 40% are coming from decays of b hadrons in $Z \to b\bar{b}$ events. To enrich the fraction of D_s^{**} mesons produced in c events further cuts are applied.
For the tracks in the opposite hemisphere of the D_s^{**} meson the probability of all tracks to come from the primary vertex is calculated. For $Z \to b\bar{b}$ events this probability (p_{hemi}) is small due to the long lifetime of b hadrons. To suppress $Z \to b\bar{b}$ events $-log_{10}(p_{hemi})$ of the opposite hemisphere has to be smaller than 3.
The energy spectrum of D_s^{**} mesons produced in the fragmentation of primary c quarks is much harder than for D_s^{**} mesons produced in the decays of b hadrons. Requiring the scaled energy of the D_s^{**} meson to be greater than 0.45 further suppresses D_s^{**} mesons produced in decays of b hadrons.
Finally it is exploited that D_s^{**} mesons produced in $Z \to c\bar{c}$ events decay close to the primary vertex and therefore D^0 mesons produced in these decays have a smaller distance to the primary vertex than D^0 mesons coming from D_s^{**} mesons produced in decays of b hadrons. In the c enriched sample the distance of the reconstructed D^0 vertex to the primary vertex has to be smaller than 0.35 cm. The distributions of scaled energy of D_s^{**} mesons, opposite hemisphere probability and D^0 distance to primary vertex for

Z$\rightarrow b\bar{b}$ and Z$\rightarrow c\bar{c}$ events are shown in Fig. 2. After applying these cuts approximately 90% of the selected D_s^{**} mesons are originating from Z$\rightarrow c\bar{c}$ events.
In Fig. 3 the mass distributions for the c enriched sample are plotted. The number of signal events is determined with the same fitting procedure as described in the previous paragraph. The results of the fits are shown in Table 6.

Decay channel	Fit results
$D_{s1}^{+}\rightarrow D^{*+}K_S^0$	$n(D_{s1}^{\pm})=9.8 \pm 3.3_{stat} \pm 0.6_{syst}$
$D_{s1}^{+}\rightarrow D^{*0}K^{+}$	$n(D_{s1}^{\pm})=18.1 \pm 6.4_{stat} \pm 2.0_{syst}$
$D_{s2}^{*+}\rightarrow D^{0}K^{+}$	$n(D_{s2}^{*\pm})=24.5 \pm 9.9_{stat} \pm 2.5_{syst}$

Table 6: Results of the fit to the ΔM_3 = m(D^0,K^+)-m(D^0) distribution in the c enriched data sample.

6 Production Rates $b \rightarrow D_s^{**}$

The specificity of Z$\rightarrow b\bar{b}$ events, namely the use of the long lifetime of the b, leads to a separate analysis. Hence, the channels used and the cuts applied are somewhat different from those defined in the previous paragraphs. The track and event selection are the same but only preselected events for years 1992-1995 are used, which corresponds to 3.7 million events.

6.1 Charmed Meson Selection

All the selected charmed mesons in the $b \rightarrow D_s^{**}$ analysis are searched in two D^0 decay modes, $D^0\rightarrow K^-\pi^+$and $D^0\rightarrow K^-\pi^+\pi^-\pi^+$. The most important cuts for the suppression of combinatorial background are related to the distance of the displaced vertex of the D^0 from the primary vertex and the probability of the tracks to come from the primary vertex.
The charged kaon candidates are selected using the dE/dx information from the TPC, as described in paragraph 2.2. However, more stringent cuts are put on r_K: the associated tracks are required to satisfy $-3 < r_K < 1.5$. All pion candidates are required to satisfy $-3 < r_\pi < 3$. For all the track candidates, if dE/dx information is not available, the track is kept in the combinations.
The charmed mesons are reconstructed using all possible combinations of pion and kaon track candidates with at least one hit in the VDET. At least two tracks are required to have VDET hits in both the $r\phi$ and z views. The overall momentum cuts are lowered compared to the $c \rightarrow D_s^{**}$ analysis to gain efficiency. Pion candidates are required to have a momentum greater than 0.5 GeV/c, whilst kaons are required to have a momentum greater than 1.6 GeV/c. For $D^0\rightarrow K^-\pi^+\pi^-\pi^+$, the lowest momentum pion threshold is lowered to 0.35 GeV/c.

The track combinations satisfying the above criteria are fit to a common vertex. The χ^2 probability of the vertex fit must be larger than 0.1%. The reconstructed D^0 vertex is required to be at least 2 mm away from the interaction point. For the decay mode $D^0 \to K^-\pi^+$, the two tracks are required to have a probability to come from the interaction point lower than 50%. For the decay mode $D^0 \to K^-\pi^+\pi^-\pi^+$, tracks of momentum $p < 3$ GeV/c which have a probability larger than 10% to come from the interaction point are discarded.
D^{*+}candidates found in the decay $D_{s1}^+ \to D^{*+}K_S^0$, have lower combinatorial background. In order to obtain such $D^{*\pm}$ candidates, one relaxes cuts on the distance of the D^0 vertex from the primary vertex (> 1 mm for $D^0 \to K^-\pi^+$), on r_K (< 2) and removes tracks probability requirements. These D^0 candidates are then used to reconstruct $D^{*\pm}$ candidates, in the channel $D^{*\pm} \to D^0\pi^\pm$. The mass difference $\Delta M_1 = m(D^0,\pi^+) - m(D^0)$ is calculated and required to be within 2 MeV/c^2 of 145.4 MeV/c^2.

6.2 Decay channel $b \to D_{s1}^+ \to D^{*0}K^+$ and $b \to D_{s2}^{*+} \to D^0K^+$

The $D_{s1}^+ \to D^{*0}K^+$ and $D_{s2}^{*+} \to D^0K^+$ were reconstructed using the same technique as described in the general analysis. The resolution for $\Delta M_3 = m(D^0,K^+) - m(D^0)$ is found to be approximately the same, (2.7 ± 0.1) MeV/c^2 for $D_{s1}^+ \to D^{*0}K^+$ where $D^{*0} \to D^0\pi^0$. In the case $D^{*0} \to D^0\gamma$, the resolution is found to be (7.8 ± 0.2) MeV/c^2 and (3.2 ± 0.1) MeV/c^2 for $D_{s2}^{*+} \to D^0K^+$.
One of the most important cuts used for the $D_{s1}^+ \to D^{*0}K^+$and $D_{s2}^{*+} \to D^0K^+$reconstruction in b decays are the ones aimed at fighting the pion background, requiring $r_K < 1$ and $|r_\pi| > 1$ for the track candidate corresponding to the kaon. The other very important cuts are the ones that enable a b/c separation. Those are the requirement for the scaled energy of the D_s^{**} to be lower than 0.6 and the already mentioned cut on the distance of the vertex of the D^0 with respect to the primary vertex. In addition, in the case $D^0 \to K^-\pi^+$, $-log(p_{hemi})$ has to be larger than 2, where p_{hemi} is the probability of all tracks in the opposite hemisphere of the D_s^{**} to come from the primary vertex.
The reconstruction efficiencies are much lower than the ones obtained in the general D_s^{**} search mainly because of the very low efficiency on $D^0 \to K^-\pi^+\pi^-\pi^+$ mode.
The mass difference distribution $\Delta M_3 = m(D^0,K^+) - m(D^0)$ obtained in the data is shown in Fig. 4. To be able to estimate the combinatorial background, all the D^0 candidates which form an invariant mass in the range $1.79 - 1.82$ GeV/c^2 or $1.9 - 1.93$ GeV/c^2 are selected and (D^0 candidate, K^+) combinations are formed. This range was chosen to obtain an approximately equal number of data and background events in the final sample, and to bias the less possible the shape of the background. The contributions from reflections from the decays $D_1^+ \to D^{*0}\pi^+$ and $D_2^{*+} \to D^0\pi^+$ are found to be negligible under the peaks and are not taken into account. As will be seen, a systematic error will be put in order to account for the uncertainty in the shape of the background. The position of the peaks was let to vary freely in the fits. Except for the previous remarks, the fitting procedure is the same as already described in the general analysis and leads to the results shown in Table 7.

Decay channel	Fit results
$D_{s1}^{+} \to D^{*0} K^{+}$	$n(D_{s1}^{\pm})=27.8 \pm 13.3_{stat} \pm 2.1_{syst}$
$D_{s2}^{*+} \to D^{0} K^{+}$	$n(D_{s2}^{*\pm})=62.0 \pm 23.0_{stat} \pm 13.3_{syst}$

Table 7: Results of the fit to the $\Delta M_3 = m(D^0,K^+) - m(D^0)$ distribution in data for $b \to D_s^{**}$ search.

6.3 Decay channel $b \to D_{s1}^{+} \to D^{*+} K_S^0$

The $D_{s1}^{+} \to D^{*+} K^0$ was reconstructed using the same technique as described in the general analysis except that only two decays, $D^0 \to K^- \pi^+$ and $D^0 \to K^- \pi^+ \pi^- \pi^+$ were used. The neutral vertices corresponding to K_S^0 candidates were required to have a distance of at least 1 cm to the primary vertex. The overall detector resolution for the $D_{s1}^{\pm}$ reconstruction was determined to be 1.3 ± 0.1 MeV/c^2.
As for the previous selection, to obtain a good b/c separation, cuts were applied on the scaled energy of the $D_{s1}^{\pm}$ candidate ($x_E < 0.6$) and on the probability of all the tracks in the opposite hemisphere to come from the primary vertex ($-log(p_{hemi}) > 2$). The mass difference distribution $\Delta M_2 = m(D^{*+},K_S^0) - m(D^{*+})$ obtained in the data is shown in Fig. 4 . Sidebands ([1.74; 1.82] GeV/c^2 and [1.9; 1.97] GeV/c^2) of the D^0 mass distributions are used to determine the combinatorial background. The position of the peak was let to vary freely during the fit procedure, which was once again the same as described in the general analysis. The result is $n(D_{s1}^{\pm} \to D^{*\pm} K^0) = 15.1 \pm 6.5_{stat} \pm 3.0_{syst}$.

7 Systematic errors

The main source of systematic error is the uncertainty in the natural width of the $D_{s1}^{\pm}$ and $D_{s2}^{*\pm}$ mesons: $\Gamma(D_{s1}^{\pm}) < 2.3$ MeV and $\Gamma(D_{s2}^{*\pm}) = 15^{+5}_{-4}$ MeV [4]. This is taken into account by varying these parameters in the fit. Other sources of systematic uncertainties are the errors on the D^0 branching ratio and the errors on the reconstruction efficiencies due to the finite number of signal Monte Carlo events.

8 Results

From the measured numbers of produced $D_{s1}^{\pm}$ and $D_{s2}^{*\pm}$ mesons and the reconstruction efficiencies the production rates in the decay channels ($D_{s1}^{+}\to D^{*+}K^{0}$), ($D_{s1}^{+}\to D^{*0}K^{+}$) and ($D_{s2}^{*+}\to D^{0}K^{+}$) in hadronic events are found to be:

$$\begin{aligned}
n(Z\to D_{s1}^{\pm})_{x_E(D_{s1}^{\pm})>0.3}\cdot Br(D_{s1}^{+}\to D^{*+}K^{0}) &= (0.16\pm 0.04_{stat}\pm 0.02_{syst})\cdot 10^{-2}\\
n(Z\to D_{s1}^{\pm})_{x_E(D_{s1}^{\pm})>0.3}\cdot Br(D_{s1}^{+}\to D^{*0}K^{+}) &= (0.25\pm 0.07_{stat}\pm 0.04_{syst})\cdot 10^{-2}\\
n(Z\to D_{s2}^{*\pm})_{x_E(D_{s2}^{*\pm})>0.3}\cdot Br(D_{s2}^{*+}\to D^{0}K^{+}) &= (0.38\pm 0.10_{stat}\pm 0.07_{syst})\cdot 10^{-2}
\end{aligned}$$

The ratio of the two D_{s1}^{+} branching ratios is:

$$\frac{Br(D_{s1}^{+}\to D^{*0}K^{+})}{Br(D_{s1}^{+}\to D^{*+}K^{0})} = 1.6\pm 0.4_{stat}\pm 0.2_{syst}$$

The enhancement of the $D^{*0}K^{+}$ final state is due to the higher Q-value of the decay since isospin invariance requires the matrix elements of the two decays to be the same. The ratio of the two branching ratios is given by the following formula:

$$R = \frac{Br(D_{s1}^{+}\to D^{*0}K^{+})}{Br(D_{s1}^{+}\to D^{*+}K^{0})} = \left(\frac{q_{D^{*0}K^{+}}}{q_{D^{*+}K^{0}}}\right)^{2L+1} \approx 1.77$$

where q is the momentum of the final state particles in the rest frame of the D_{s1}^{+} and L=2 for a pure D-Wave decay. The measured ratio agrees very well with the expected value.

From the observed number of D_s^{**} mesons in the c enriched sample the production rates ($c\to D_s^{**}$) in the three observed decay channels are found to be:

$$\begin{aligned}
n(c\to D_{s1}^{\pm})\cdot Br(D_{s1}^{+}\to D^{*+}K^{0}) &= (0.27\pm 0.09_{stat}\pm 0.02_{syst})\cdot 10^{-2}\\
n(c\to D_{s1}^{\pm})\cdot Br(D_{s1}^{+}\to D^{*0}K^{+}) &= (0.51\pm 0.18_{stat}\pm 0.06_{syst})\cdot 10^{-2}\\
n(c\to D_{s2}^{*\pm})\cdot Br(D_{s2}^{*+}\to D^{0}K^{+}) &= (0.58\pm 0.24_{stat}\pm 0.06_{syst})\cdot 10^{-2}
\end{aligned}$$

From the observed number of D_s^{**} mesons in the b enriched sample the production rates ($b\to D_s^{**}$) in the three observed decay channels are found to be:

$$\begin{aligned}
n(b\to D_{s1}^{\pm})\cdot Br(D_{s1}^{+}\to D^{*+}K^{0}) &= (0.48\pm 0.21_{stat}\pm 0.11_{syst})\cdot 10^{-2}\\
n(b\to D_{s1}^{\pm})\cdot Br(D_{s1}^{+}\to D^{*0}K^{+}) &= (0.57\pm 0.27_{stat}\pm 0.08_{syst})\cdot 10^{-2}\\
n(b\to D_{s2}^{*\pm})\cdot Br(D_{s2}^{*+}\to D^{0}K^{+}) &= (1.0\pm 0.4_{stat}\pm 0.2_{syst})\cdot 10^{-2}
\end{aligned}$$

Assuming that the decay width of the D_{s1}^{+} is saturated by the two measured decays and that the branching ratio $D_{s2}^{*+} \to D^0 K^+$ is 45% the total production rates in hadronic events are:

$$n(Z \to D_{s1}^{\pm})_{x_E(D_{s1}^{\pm})>0.3} = (0.41 \pm 0.08_{stat} \pm 0.06_{syst}) \cdot 10^{-2}$$
$$n(Z \to D_{s2}^{*\pm})_{x_E(D_{s2}^{*\pm})>0.3} = (0.84 \pm 0.22_{stat} \pm 0.15_{syst}) \cdot 10^{-2}$$

The production rates from c quarks ($c \to D_s^{**}$) are:

$$n(c \to D_{s1}^{\pm}) = (0.77 \pm 0.20_{stat} \pm 0.08_{syst}) \cdot 10^{-2}$$
$$n(c \to D_{s2}^{*\pm}) = (1.3 \pm 0.5_{stat} \pm 0.2_{syst}) \cdot 10^{-2}$$

The production rates from b quarks ($b \to D_s^{**}$) are:

$$n(b \to D_{s1}^{\pm}) = (1.1 \pm 0.3_{stat} \pm 0.2_{syst}) \cdot 10^{-2}$$
$$n(b \to D_{s2}^{*\pm}) = (2.2 \pm 0.8_{stat} \pm 0.5_{syst}) \cdot 10^{-2}$$

References

[1] ARGUS Collaboration, *Observation of the decay* $D_{s1}(2536) \to D^{*0}K^{+}$, Physics Letters B 297 (1992) 425-431

[2] CLEO Collaboration, *Production and decay of the* $D_{s1}(2536)^{+}$, Physics Letters B 303 (1993) 377-384

[3] CLEO Collaboration, *Observation of a New Charmed Strange Meson*, Physical Review Letters Vol 72 Number 13 (1994) 377-384

[4] Particle Data Group, *Review of Particle Properties,* Physical Review D54,1 (1996)

[5] The Opal Collaboration, *Production of P-Wave Charm and Charm-Strange Mesons in Hadronic* Z^0 *Decays,* Zeitschift fuer Physik C 76 (1997) 425-440

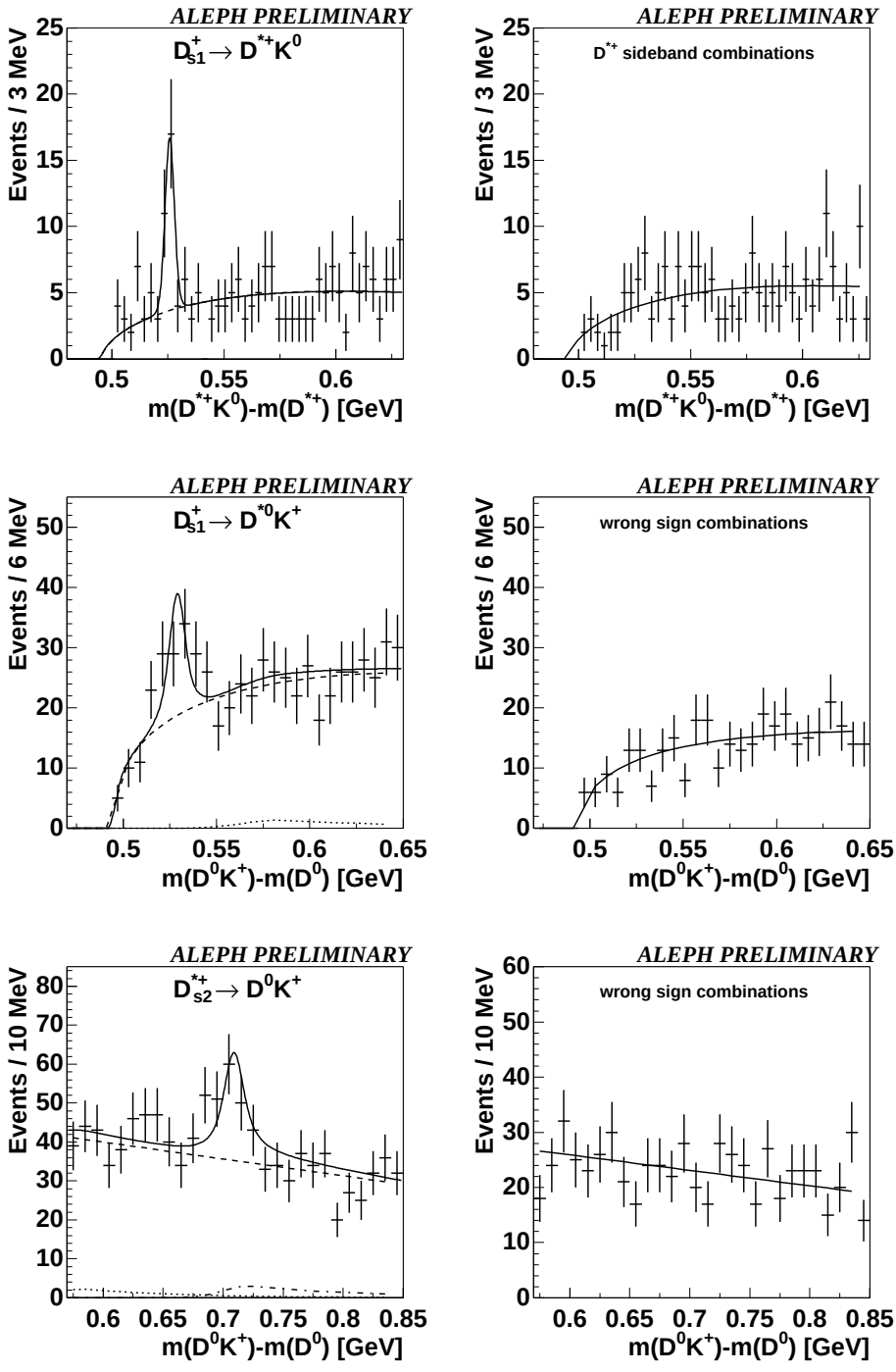

Figure 1: The plots show the mass distribution for the reconstruction of $D_{s1}^{+} \to D^{*+}K^{0}$, $D_{s1}^{+} \to D^{*0}K^{+}$ and $D_{s2}^{*+} \to D^{0}K^{+}$ decays. The background is determined with the help of $D^{*\pm}$ candidates from the sidebands and wrong-sign combinations (D^{0}, K^{-}). The dashed lines shows the combinatorial background and the dotted line shows the contribution of reflections from $D_1 \to D^{*0}\pi^{+}$ and $D_2^{*} \to D^{0}\pi^{+}$ decays determined from Monte Carlo.

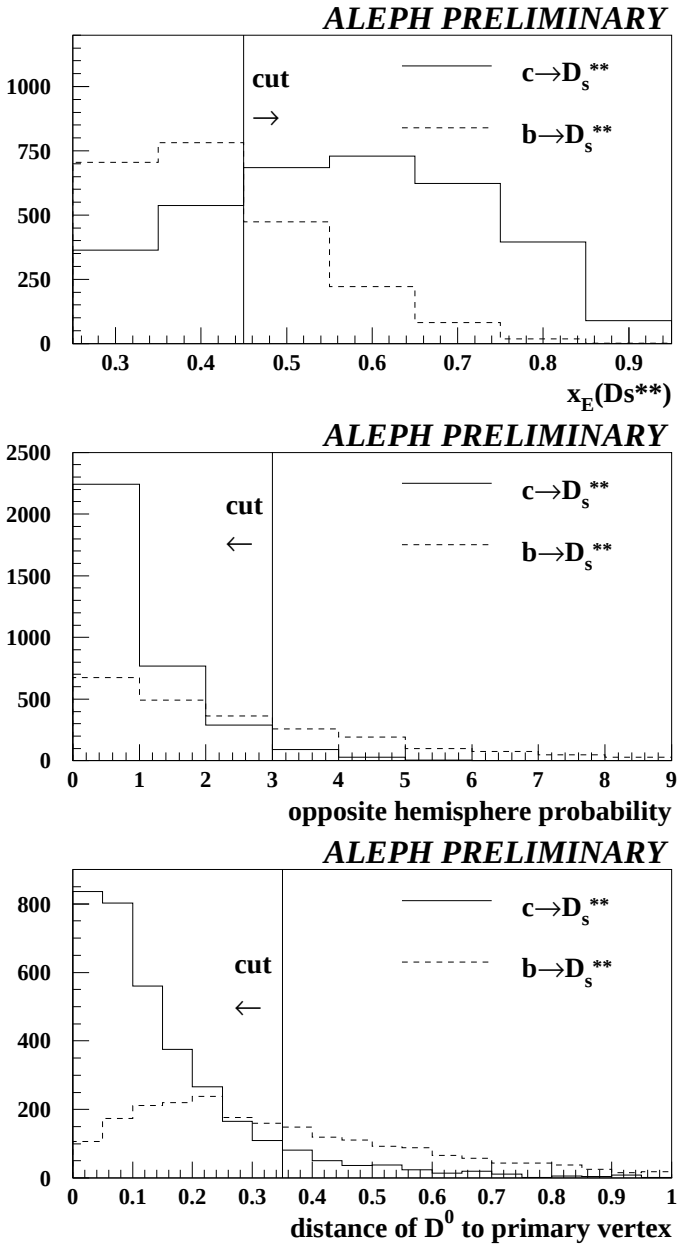

Figure 2: Distributions of the scaled energy of D_s^{**} mesons, opposite hemisphere probability and the distance of D^0 mesons to the primary vertex for $Z \to c\bar{c}$ and $Z \to b\bar{b}$ events obtained from Monte Carlo. The cuts for the suppression of D_s^{**} mesons from $Z \to b\bar{b}$ events are marked.

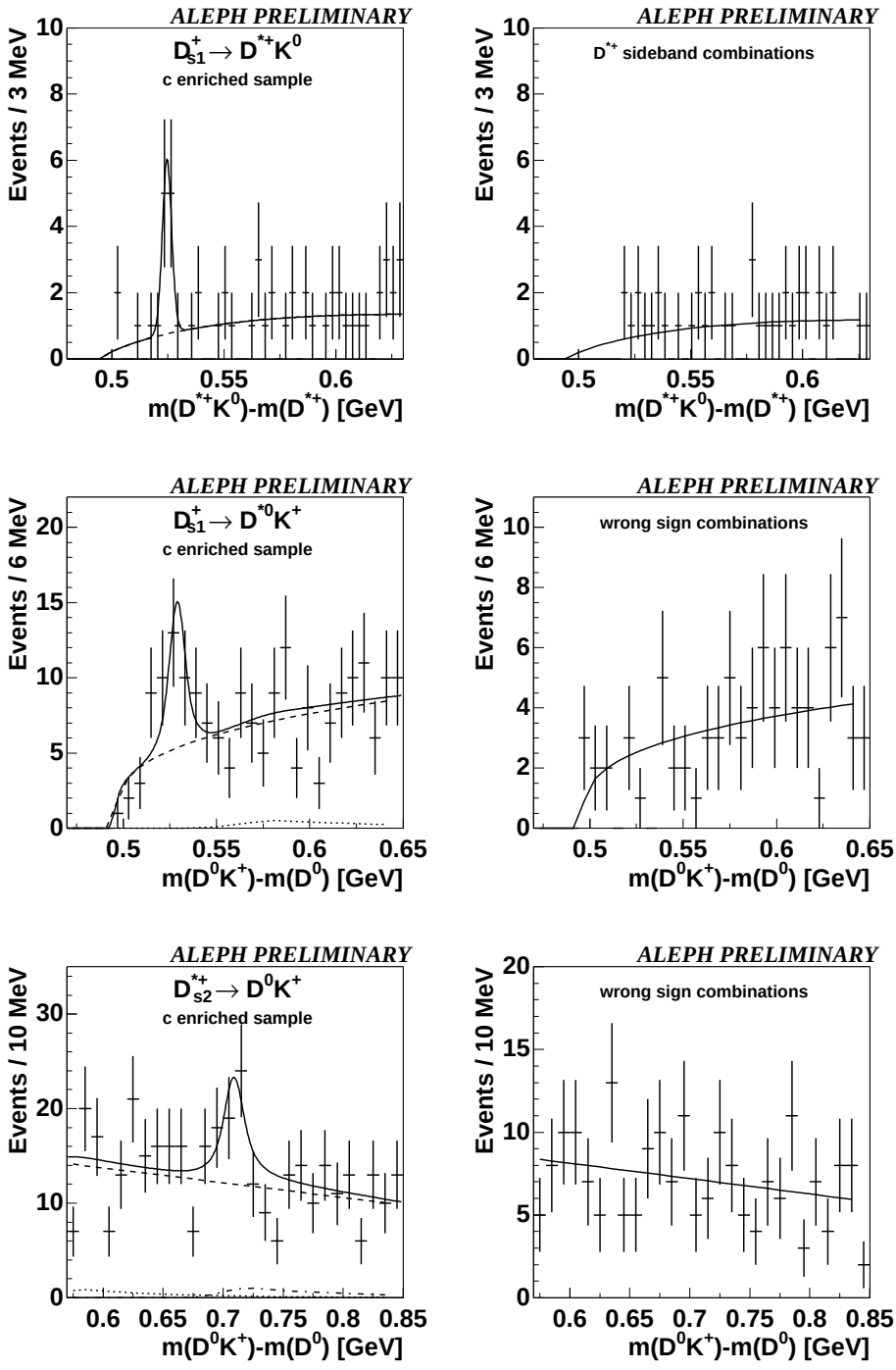

Figure 3: Mass distribution for the reconstruction of $D_{s1}^{+} \to D^{*+}K^{0}$, $D_{s1}^{+} \to D^{*0}K^{+}$ and $D_{s2}^{*+} \to D^{0}K^{+}$ decays in the c enriched sample. The background is determined with the help of combinations with D^{*+} candidates from the sidebands and wrong-sign combinations (D^{0}, K^{-}). The dashed lines shows the combinatorial background and the dotted line shows the contribution of reflections from $D_1 \to D^{*0}\pi^{+}$ and $D_2^{*} \to D^{0}\pi^{+}$ decays determined from Monte Carlo.

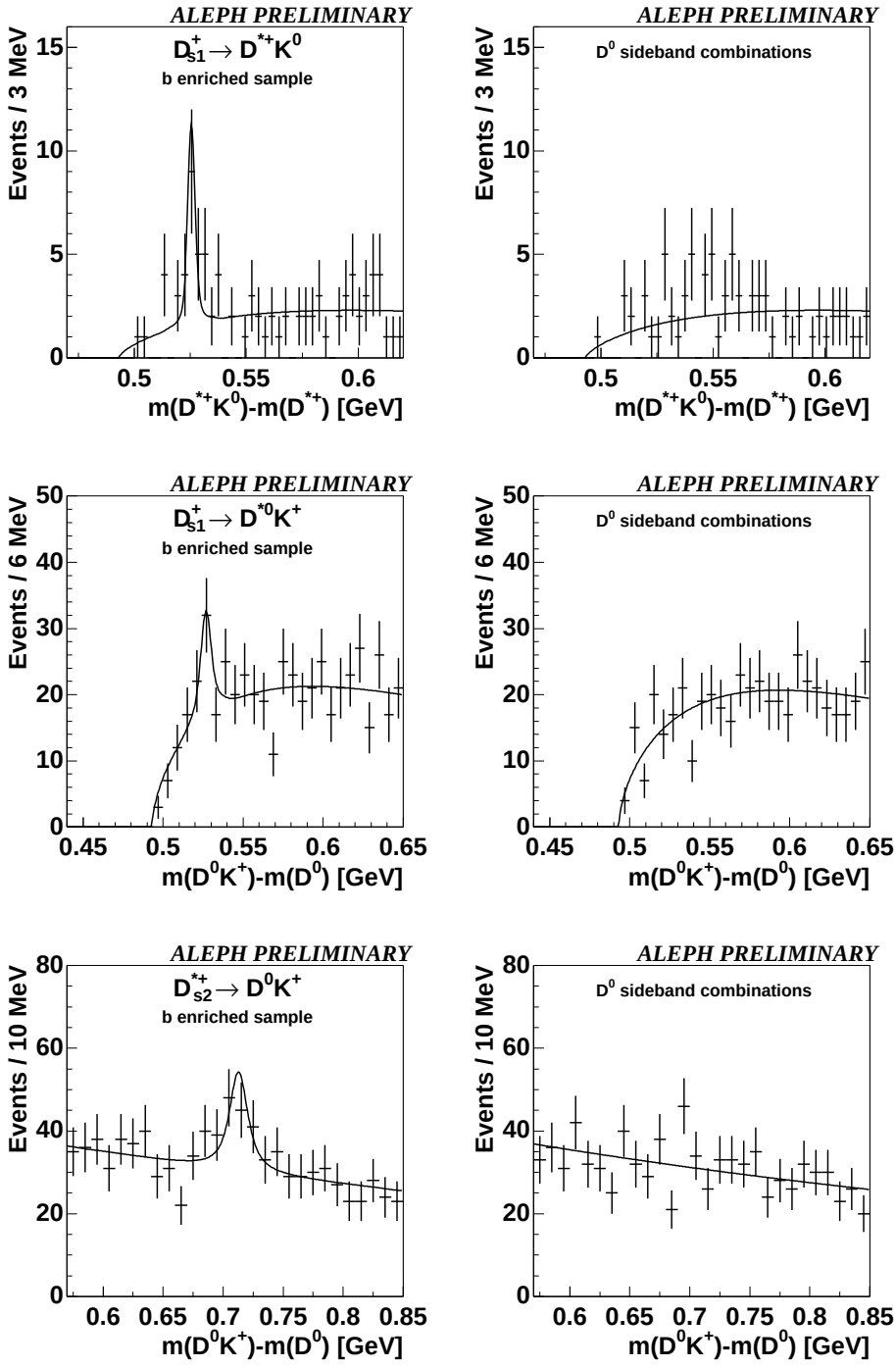

Figure 4: Mass distribution for the reconstruction of $D_{s1}^{+} \to D^{*+}K^{0}$, $D_{s1}^{+} \to D^{*0}K^{+}$ and $D_{s2}^{*+} \to D^{0}K^{+}$ decays in the b enriched sample. The background is determined with the help of combinations with D^{0} candidates from the sidebands